EUROPEAN ORGANIZATION FOR NUCLEAR RESEARCH

CERN-PPE/91-109

5 July 1991

The Reaction $e^+e^- \to \gamma\gamma(\gamma)$ at Z^o Energies

DELPHI Collaboration

Abstract

The total and differential cross-sections for the reaction $e^+e^- \to \gamma\gamma(\gamma)$ are measured at centre of mass energies around 91 GeV using an integrated luminosity of $4.7pb^{-1}$. The agreement with the QED prediction is good. Consequently there is no evidence for non-standard channels which would have the same experimental signature. The lower limits on the QED cutoff parameters are $\Lambda_+ > 113$ GeV and $\Lambda_- > 95$ GeV. An upper limit on the effective coupling between a possible excited electron and the gamma is derived. At 95% confidence level the branching ratios for Z^0 decay into $\pi^0\gamma$, $\eta\gamma$ and $\gamma\gamma\gamma$ are below 1.5×10^{-4}, 2.8×10^{-4} and 1.4×10^{-4} respectively.

(Submitted to Physics Letters B)

P.Abreu[16], W.Adam[42], F.Adami[33], T.Adye[31], T.Akesson[19], G.D.Alekseev[12], P.Allen[41], S.Almehed[19], F.Alted[41], S.J.Alvsvaag[4], U.Amaldi[7], E.Anassontzis[3], P.Antilogus[20], W-D.Apel[13], R.J.Apsimon[31], B.Åsman[37], P.Astier[16], J-E.Augustin[15], A.Augustinus[7], P.Baillon[7], P.Bambade[15], F.Barao[16], G.Barbiellini[39], D.Y.Bardin[12], A.Baroncelli[34], O.Barring[19], W.Bartl[42], M.Battaglia[24], M.J.Bates[29], M.Baubillier[16], K-H.Becks[44], C.J.Beeston[29], M.Begalli[10], P.Beilliere[6], Yu.Belokopytov[36], P.Beltran[9], D.Benedic[8], J.M.Benlloch[41], M.Berggren[37], D.Bertrand[2], S.Biagi[17], F.Bianchi[38], J.H.Bibby[29], M.S.Bilenky[12], P.Billoir[16], J.Bjarne[19], D.Bloch[8], S.Blyth[29], P.N.Bogolubov[12], T.Bolognese[33], M.Bonapart[26], M.Bonesini[24], W.Bonivento[24], P.S.L.Booth[17], M.Boratav[16], P.Borgeaud[33], G.Borisov[36], H.Borner[29], C.Bosio[34], O.Botner[40], B.Bouquet[15], M.Bozzo[10], S.Braibant[7], P.Branchini[34], K.D.Brand[30], R.A.Brenner[11], C.Bricman[2], R.C.A.Brown[7], N.Brummer[26], J-M.Brunet[6], L.Bugge[28], T.Buran[28], H.Burmeister[7], J.A.M.A.Buytaert[2], M.Caccia[7], M.Calvi[24], A.J.Camacho Rozas[35], J-E.Campagne[7], A.Campion[17], T.Camporesi[7], V.Canale[32], F.Cao[2], L.Carroll[17], C.Caso[10], E.Castelli[39], M.V.Castillo Gimenez[41], A.Cattai[7], F.R.Cavallo[5], L.Cerrito[32], P.Charpentier[7], P.Checchia[30], G.A.Chelkov[12], L.Chevalier[33], P.Chliapnikov[36], V.Chorowicz[18], R.Cirio[38], M.P.Clara[38], P.Collins[29], J.L.Contreras[21], R.Contri[10], G.Cosme[15], F.Couchot[15], H.B.Crawley[1], D.Crennell[31], G.Crosetti[10], N.Crosland[29], M.Crozon[8], J.Cuevas Maestro[35], S.Czellar[11], S.Dagoret[15], E.Dahl-Jensen[25], B.Dalmagne[15], M.Dam[7], G.Damgaard[25], G.Darbo[10], E.Daubie[2], P.D.Dauncey[29], M.Davenport[7], P.David[16], A.De Angelis[39], M.De Beer[33], H.De Boeck[2], W.De Boer[13], C.De Clercq[2], M.D.M.De Fez Laso[41], N.De Groot[26], C.De La Vaissiere[16], B.De Lotto[39], A.De Min[24], C.Defoix[6], D.Delikaris[7], S.Delorme[7], P.Delpierre[8], N.Demaria[38], J.Derkaoui[38,22], L.Di Ciaccio[32], H.Dijkstra[7], F.Djama[8], J.Dolbeau[6], M.Donszelmann[26], K.Doroba[43], M.Dracos[7], J.Drees[44], M.Dris[27], Y.Dufour[6], W.Dulinski[8], R.Dzhelyadin[36], L-O.Eek[40], P.A.-M.Eerola[11], T.Ekelof[40], G.Ekspong[37], A.Elliot Peisert[30], J-P.Engel[8], D.Fassouliotis[27], A.Fenyuk[36], M.Fernandez Alonso[35], A.Ferrer[41], T.A.Filippas[27], A.Firestone[1], H.Foeth[7], E.Fokitis[27], P.Folegati[39], F.Fontanelli[10], H.Forsbach[44], B.Franek[31], P.Frenkiel[6], D.C.Fries[13], A.G.Frodesen[4], R.Fruhwirth[42], F.Fulda-Quenzer[15], K.Furnival[17], H.Furstenau[13], J.Fuster[7], J.M.Gago[16], G.Galeazzi[30], D.Gamba[38], C.Garcia[41], J.Garcia[35], U.Gasparini[30], P.Gavillet[7], E.N.Gazis[27], J-P.Gerber[8], P.Giacomelli[5], K-W.Glitza[44], R.Gokieli[7], V.M.Golovatyuk[12], J.J.Gomez Y Cadenas[7], A.Goobar[37], G.Gopal[31], M.Gorski[43], V.Gracco[10], A.Grant[7], F.Grard[2], E.Graziani[34], M-H.Gros[15], G.Grosdidier[15], B.Grossetete[18], S.Gumenyuk[36], J.Guy[31], F.Hahn[7], M.Hahn[13], S.Haider[26], Z.Hajduk[26], A.Hakansson[19], A.Hallgren[40], K.Hamacher[44], G.Hamel De Monchenault[33], F.J.Harris[29], B.W.Heck[7], I.Herbst[44], J.J.Hernandez[41], P.Herquet[2], H.Herr[7], I.Hietanen[11], E.Higon[41], H.J.Hilke[7], S.D.Hodgson[29], T.Hofmokl[43], R.Holmes[1], S-O.Holmgren[37], D.Holthuizen[26], P.F.Honore[6], J.E.Hooper[25], M.Houlden[17], J.Hrubec[42], P.O.Hulth[37], K.Hultqvist[37], D.Husson[8], B.D.Hyams[7], P.Ioannou[3], D.Isenhower[7], P-S.Iversen[4], J.N.Jackson[17], P.Jalocha[14], G.Jarlskog[19], P.Jarry[33], B.Jean-Marie[15], E.K.Johansson[37], D.Johnson[17], M.Jonker[7], L.Jonsson[19], P.Juillot[8], G.Kalkanis[3], G.Kalmus[31], G.Kantardjian[7], F.Kapusta[18], A.Katargin[36], S.Katsanevas[3], E.C.Katsoufis[27], R.Keranen[11], J.Kesteman[2], B.A.Khomenko[12], N.N.Khovanski[12], B.King[17], N.J.Kjaer[25], H.Klein[7], W.Klempt[7], A.Klovning[4], P.Kluit[26], J.H.Koehne[13], B.Koene[26], P.Kokkinias[9], M.Kopf[13], M.Koratzinos[7], K.Korcyl[14], A.V.Korytov[12], B.Korzen[7], V.Kostukhin[36], C.Kourkoumelis[3], T.Kreuzberger[42], J.Krolikowski[43], U.Kruener-Marquis[44], W.Krupinski[14], W.Kucewicz[24], K.Kurvinen[11], C.Lacasta[41], C.Lambropoulos[9], J.W.Lamsa[1], L.Lanceri[39], V.Lapin[36], J-P.Laugier[33], R.Lauhakangas[11], G.Leder[42], F.Ledroit[6], J.Lemonne[2], G.Lenzen[44], V.Lepeltier[15], A.Letessier-Selvon[18], D.Liko[42], E.Lieb[44], E.Lillethun[4], J.Lindgren[11], A.Lipniacka[43], I.Lippi[30], R.Llosa[21], B.Loerstad[19], M.Lokajicek[12], J.G.Loken[29], M.A.Lopez Aguera[35], A.Lopez-Fernandez[15], M.Los[26], D.Loukas[9], A.Lounis[8], J.J.Lozano[41], R.Lucock[31], P.Lutz[6], L.Lyons[29], G.Maehlum[7], J.Maillard[6], A.Maltezos[9], S.Maltezos[27], F.Mandl[42], J.Marco[35], M.Margoni[30], J-C.Marin[7], A.Markou[9], S.Marti[41], L.Mathis[6], F.Matorras[35], C.Matteuzzi[24], G.Matthiae[32], M.Mazzucato[30], M.Mc Cubbin[17], R.Mc Kay[1], R.Mc Nulty[17], E.Menichetti[38], C.Meroni[24], W.T.Meyer[1], M.Michelotto[30], W.A.Mitaroff[42], G.V.Mitselmakher[12], U.Mjoernmark[19], T.Moa[37], R.Moeller[25], K.Moenig[44], M.R.Monge[10], P.Morettini[10], H.Mueller[13], H.Muller[7], W.J.Murray[31], G.Myatt[29], F.Naraghi[18], U.Nau-Korzen[44], F.L.Navarria[5], P.Negri[24], B.S.Nielsen[25], B.Nijjhar[17], V.Nikolaenko[36], V.Obraztsov[36], A.G.Olshevski[12], R.Orava[11], A.Ostankov[36], A.Ouraou[33], R.Pain[18], H.Palka[26], T.Papadopoulou[27], L.Pape[7], A.Passeri[34], M.Pegoraro[30], V.Perevoschikov[36], M.Pernicka[42], A.Perrotta[5], F.Pierre[33], M.Pimenta[16], O.Pingot[2], A.Pinsent[29], M.E.Pol[16], G.Polok[14], P.Poropat[39], P.Privitera[13], A.Pullia[24], J.Pyyhtia[11], D.Radojicic[29], S.Ragazzi[24], W.H.Range[17], P.N.Ratoff[29], A.L.Read[28], N.G.Redaelli[24], M.Regler[42], D.Reid[17], P.B.Renton[29], L.K.Resvanis[3], F.Richard[15], M.Richardson[17], J.Ridky[12], G.Rinaudo[38], I.Roditi[7], A.Romero[38], I.Roncagliolo[10], P.Ronchese[30], C.Ronnqvist[11], E.I.Rosenberg[1], U.Rossi[5], E.Rosso[7], P.Roudeau[15], T.Rovelli[5], W.Ruckstuhl[26], V.Ruhlmann[33], A.Ruiz[35], K.Rybicki[14], H.Saarikko[11], Y.Sacquin[33], J.Salt[41], E.Sanchez[41], J.Sanchez[21], M.Sannino[10], M.Schaeffer[8], S.Schael[13], H.Schneider[13], F.Scuri[39], A.M.Segar[29], R.Sekulin[31], M.Sessa[39], G.Sette[10], R.Seufert[13], R.C.Shellard[16], P.Siegrist[33], S.Simonetti[10], F.Simonetto[30], A.N.Sissakian[12], T.B.Skaali[28], G.Skjevling[28], G.Smadja[33,20], G.R.Smith[31], R.Sosnowski[43], T.S.Spassoff[12], E.Spiriti[34], S.Squarcia[10], H.Staeck[44], C.Stanescu[34], G.Stavropoulos[9], F.Stichelbaut[2], A.Stocchi[15], J.Strauss[42],

R.Strub[8], C.J.Stubenrauch[7], M.Szczekowski[43], M.Szeptycka[43], P.Szymanski[43], T.Tabarelli[24], S.Tavernier[2], G.E.Theodosiou[9], A.Tilquin[23], J.Timmermans[26], V.G.Timofeev[12], L.G.Tkatchev[12], T.Todorov[12], D.Z.Toet[26], L.Tortora[34], M.T.Trainor[29], D.Treille[7], U.Trevisan[10], W.Trischuk[7], G.Tristram[6], C.Troncon[24], A.Tsirou[7], E.N.Tsyganov[12], M.Turala[14], R.Turchetta[8], M-L.Turluer[33], T.Tuuva[11], I.A.Tyapkin[12], M.Tyndel[31], S.Tzamarias[7], B.Ueberschaer[44], S.Ueberschaer[44], O.Ullaland[7], V.A.Uvarov[36], G.Valenti[5], E.Vallazza[38], J.A.Valls Ferrer[41], G.W.Van Apeldoorn[26], P.Van Dam[26], W.K.Van Doninck[2], N.Van Eijndhoven[7], C.Vander Velde[2], J.Varela[16], P.Vaz[16], G.Vegni[24], J.Velasco[41], L.Ventura[30], W.Venus[31], F.Verbeure[2], L.S.Vertogradov[12], L.Vibert[18], D.Vilanova[33], E.V.Vlasov[36], A.S.Vodopyanov[12], M.Vollmer[44], S.Volponi[5], G.Voulgaris[3], M.Voutilainen[11], V.Vrba[34], H.Wahlen[44], C.Walck[37], F.Waldner[39], M.Wayne[1], P.Weilhammer[7], J.Werner[44], A.M.Wetherell[7], J.H.Wickens[2], J.Wikne[28], G.R.Wilkinson[29], W.S.C.Williams[29], M.Winter[8], D.Wormald[28], G.Wormser[15], K.Woschnagg[40], N.Yamdagni[37], P.Yepes[7], A.Zaitsev[36], A.Zalewska[14], P.Zalewski[43], E.Zevgolatakos[9], G.Zhang[44], N.I.Zimin[12], M.Zito[33], R.Zitoun[18], R.Zukanovich Funchal[6], G.Zumerle[30], J.Zuniga[41]

[1] Ames Laboratory and Department of Physics, Iowa State University, Ames IA 50011, USA
[2] Physics Department, Univ. Instelling Antwerpen, Universiteitsplein 1, B-2610 Wilrijk, Belgium
and IIHE, ULB-VUB, Pleinlaan 2, B-1050 Brussels, Belgium
and Service de Phys. des Part. Elém., Faculté des Sciences, Université de l'Etat Mons, Av. Maistriau 19, B-7000 Mons, Belgium
[3] Physics Laboratory, University of Athens, Solonos Str. 104, GR-10680 Athens, Greece
[4] Department of Physics, University of Bergen, Allégaten 55, N-5007 Bergen, Norway
[5] Dipartimento di Fisica, Università di Bologna and INFN, Via Irnerio 46, I-40126 Bologna, Italy
[6] Collège de France, Lab. de Physique Corpusculaire, 11 pl. M. Berthelot, F-75231 Paris Cedex 05, France
[7] CERN, CH-1211 Geneva 23, Switzerland
[8] Division des Hautes Energies, CRN - Groupe DELPHI and LEPSI, B.P.20 CRO, F-67037 Strasbourg Cedex, France
[9] Institute of Nuclear Physics, N.C.S.R. Demokritos, P.O. Box 60228, GR-15310 Athens, Greece
[10] Dipartimento di Fisica, Università di Genova and INFN, Via Dodecaneso 33, I-16146 Genova, Italy
[11] Research Institute for High Energy Physics, University of Helsinki, Siltavuorenpenger 20 C, SF-00170 Helsinki 17, Finland
[12] Joint Institute for Nuclear Research, Dubna, Head Post Office, P.O. Box 79, 101 000 Moscow, USSR.
[13] Institut für Experimentelle Kernphysik, Universität Karlsruhe, Postfach 6980, D-7500 Karlsruhe 1, FRG
[14] High Energy Physics Laboratory, Institute of Nuclear Physics, Ul. Kawiory 26 a, PL-30055 Krakow 30, Poland
[15] Université de Paris-Sud, Lab. de l'Accélérateur Linéaire, Bat 200, F-91405 Orsay, France
[16] LIP, Av. Elias Garcia 14 - 1e, P-1000 Lisbon Codex, Portugal
[17] Department of Physics, University of Liverpool, P.O. Box 147, GB - Liverpool L69 3BX, UK
[18] LPNHE, Universités Paris VI et VII, Tour 33 (RdC), 4 place Jussieu, F-75230 Paris Cedex 05, France
[19] Department of Physics, University of Lund, Sölvegatan 14, S-22363 Lund, Sweden
[20] Université Claude Bernard de Lyon, 43 Bd du 11 Novembre 1918, F-69622 Villeurbanne Cedex, France
[21] Departamento de Fisica Atomica Molecular y Nuclear, Universidad Complutense, Avda. Complutense s/n, E-28040 Madrid, Spain
[22] Permanent address: Département de Physique, Faculté des Sciences d'Oujda, Maroc
[23] Faculté des Sciences de Luminy, Univ. d'Aix - Marseille II Case 907 - 70, route Léon Lachamp, F-13288 Marseille Cedex 09, France
[24] Dipartimento di Fisica, Università di Milano and INFN, Via Celoria 16, I-20133 Milan, Italy
[25] Niels Bohr Institute, Blegdamsvej 17, DK-2100 Copenhagen 0, Denmark
[26] NIKHEF-H, Postbus 41882, NL-1009 DB Amsterdam, The Netherlands
[27] National Technical University, Physics Department, Zografou Campus, GR-15773 Athens, Greece
[28] Physics Department, University of Oslo, Blindern, N-1000 Oslo 3, Norway
[29] Nuclear Physics Laboratory, University of Oxford, Keble Road, GB - Oxford OX1 3RH, UK
[30] Dipartimento di Fisica, Università di Padova and INFN, Via Marzolo 8, I-35131 Padua, Italy
[31] Rutherford Appleton Laboratory, Chilton, GB - Didcot OX11 OQX, UK
[32] Dipartimento di Fisica, Università di Roma II and INFN, Tor Vergata, I-00173 Rome.
[33] CEN-Saclay, DPhPE, F-91191 Gif-sur-Yvette Cedex, France
[34] Istituto Superiore di Sanità, Ist. Naz. di Fisica Nucl. (INFN), Viale Regina Elena 299, I-00161 Rome, Italy
[35] Facultad de Ciencias, Universidad de Santander, av. de los Castros, E - 39005 Santander, Spain
[36] Inst. for High Energy Physics, Serpukow P.O. Box 35, Protvino, (Moscow Region), USSR.
[37] Institute of Physics, University of Stockholm, Vanadisvägen 9, S-113 46 Stockholm, Sweden
[38] Dipartimento di Fisica Sperimentale, Università di Torino and INFN, Via P. Giuria 1, I-10125 Turin, Italy
[39] Dipartimento di Fisica, Università di Trieste and INFN, Via A. Valerio 2, I-34127 Trieste, Italy
and Istituto di Fisica, Università di Udine, I-33100 Udine, Italy
[40] Department of Radiation Sciences, University of Uppsala, P.O. Box 535, S-751 21 Uppsala, Sweden
[41] Inst. de Fisica Corpuscular IFIC, Centro Mixto Univ. de Valencia-CSIC, Avda. Dr. Moliner 50, E-46100 Burjassot (Valencia), Spain
[42] Institut für Hochenergiephysik, Österreich Akad. d. Wissensch., Nikolsdorfergasse 18, A-1050 Vienna, Austria
[43] Inst. Nuclear Studies and, University of Warsaw, Ul. Hoza 69, PL-00681 Warsaw, Poland
[44] Fachbereich Physik, University of Wuppertal, Postfach 100 127, D-5600 Wuppertal 1, FRG

1 Introduction

The reaction $e^+e^- \rightarrow \gamma\gamma(\gamma)$ is well suited to test QED at LEP energies and to detect the presence of non standard physics.

The QED contribution to $e^+e^- \rightarrow \gamma\gamma(\gamma)$ proceeds through the exchange of a virtual electron in the t channel. The cross section is small at these energies, typically 20 pb for polar angles greater than 40^0, compared to a total cross section of 29 nb at the Z^0 peak with the same angular acceptance. Weak radiative corrections are negligible.

The direct decay of the Z^0 into $\gamma\gamma$ is forbidden by the Landau-Yang theorem[1]. However the Z^0 decay into $\pi^0\gamma$ or $\eta\gamma$ with η decaying into neutrals would have the same experimental signature. The importance of these channels has been discussed in recent publications [2]. Measuring the $e^+e^- \rightarrow \gamma\gamma(\gamma)$ cross section either as a function of the centre of mass energy or as a function of the polar angle can distinguish these Z^0 decays from the QED contribution. The Z^0 decays would follow the resonant Z^0 line shape and have an angular distribution proportional to $(1 + cos^2\theta)$ [2], the QED process has a non resonant behaviour and is strongly peaked forward.

A search for compositeness can be made by looking either for an anomalous behaviour of the differential cross section of $e^+e^- \rightarrow \gamma\gamma$, induced by an excited electron exchanged in the t channel [3], or for an enhancement of the $e^+e^- \rightarrow \gamma\gamma\gamma$ cross section, which could signal the existence of a composite Z^0 [4].

Preliminary results on some of these channels have been presented earlier [5].

2 Apparatus

A detailed description of the DELPHI detector, of the triggering conditions and of the readout chain can be found in ref. [6]. The present analysis relies mainly on the measurement of the electromagnetic clusters in the electromagnetic calorimeters, namely the High density Projection Chamber (HPC) in the barrel and the Forward Electromagnetic Calorimeter (FEMC) in the end-caps, and on the capability of vetoing charged particle tracks using the Time Projection Chamber (TPC) and the Inner Detector (ID). The Hadron Calorimeter (HCAL) is used to veto cosmic events.

The ID is a cylindrical jet chamber covering polar angles between 20^0 and 160^0 and surrounded by 5 layers of proportional chambers. The jet chamber provides up to 24 $r\phi$ coordinates and is divided in 24 azimuthal sectors. The TPC is a cylinder with 30 cm inner radius and 122 cm outer radius and a length of 2.7 m. It is divided azimuthally into 6 sectors; there are small dead regions between the sectors. For polar angles between 25^0 and 155^0 at least 4 space points are available for track reconstruction, while for angles between 39^0 and 141^0 up to 16 space points can be used.

The HPC is a high granularity lead/gas calorimeter covering polar angles from 40^0 to 140^0. It has a segmentation in depth of nine layers. For fast triggering purposes a scintillation layer is installed after the first 5 radiation lengths of lead. The FEMC consists of 2 x 4500 lead glass blocks (granularity 1^0 x 1^0) covering polar angles from 10^0 to 36^0 and from 144^0 to 170^0. The HCAL is a sampling gas detector incorporated in the

iron magnet yoke, the barrel part covering polar angles between 43^0 and 137^0 and the two end-caps covering polar angles of 11^0 to 48^0 and 132^0 to 169^0.

The barrel neutral trigger is based on the HPC counters and the forward neutral trigger on the FEMC signals.

The luminosity measurement relies on the detection of small angle Bhabha events in the small angle tagger calorimeter (SAT). A detailed description of this measurement can be found in ref. [7].

3 Event Analysis

All the data with the electromagnetic calorimeters and the TPC fully operational collected during 1990 were used in this analysis. The integrated luminosities used in the barrel and in the forward region were 4.7 pb^{-1} and 3.7 pb^{-1} respectively.

Events with at least 2 energetic electromagnetic clusters and no tracks pointing to the vertex were selected as $\gamma\gamma(\gamma)$ candidates.

The selection criteria were the following:

- At least two clusters with energy greater than 15 GeV in the HPC ($42^0 < \theta < 88^0$ or $92^0 < \theta < 138^0$) or in the upper part of the FEMC ($29^0 < \theta < 35^0$ or $145^0 < \theta < 151^0$) with a minimum angular separation of 15^0 are required. The lower theta limit is a safe cut to ensure a high TPC efficiency.
- Events where one or both of the two most energetic electromagnetic clusters (HPC or FEMC) were close to the TPC sector boundaries were excluded ($\pm 1.5^0$ in the barrel region, $\pm 2.5^0$ in the forward region). This cut ensures high efficiency for detecting and reconstructing any associated charged particle tracks in the TPC.
- No charged particle tracks reconstructed in the TPC pointing to the vertex, and no space points in the ID aligned with the electromagnetic clusters should exist.
- Electromagnetic clusters, other than the two most energetic ones, must have an energy greater than 1 GeV in the HPC or greater than 3 GeV in the FEMC, and an angle with the the nearest accepted gamma (isolation angle) greater than 10^0 to be considered as additional gammas.

A sample of 65 events satisfied these criteria, 58 in the barrel and 7 in the forward region. All the events were visually examined. One event which had TPC tracks not pointing to the vertex and some hadronic energy in the HCAL was classified as a cosmic event. Two events had three energetic clusters in the electromagnetic calorimeters and were compatible with a three body final state. These two events were classified as $\gamma\gamma\gamma$ events. All the other events had only two visible photons and an acoplanarity (acollinearity in the plane transverse to the beam) less than 2^0 and were classified as $\gamma\gamma$ events. The same acoplanarity criteria were also applied to the Monte-Carlo events.

The separation between the selected $\gamma\gamma$ events and the Bhabha events can be seen in fig. 1, where the difference $(180^0 - \Delta\phi)$ in azimuthal angle between the two most energetic clusters is shown for both the barrel and the forward region. The acollinearity and acoplanarity distributions of the selected events (barrel and forward) are shown in fig. 2.

A precise knowledge of the photon conversion probability in front of and inside the TPC is important in order to calculate the selection efficiency. This probability has been estimated for each $cos(\theta)$ bin from the fraction of Bhabha events which are accompanied by a collinear e^+e^-pair. These events are produced in a two-step process: the outgoing electron (positron) radiates a photon through bremsstrahlung , and the photon then converts before the TPC into an e^+e^- pair seen in the detector. This method is very precise since the probability to have one such event varies quadratically with the effective number of radiation lengths; it also has a small statistical uncertainty, being based on a total of 3000 events. Several systematic effects have been taken into account. It has been checked that the result does not depend significantly on the minimum momentum of the pair; varying the momentum cut from 100 MeV to 1 GeV, the value obtained for the effective number of radiation lengths changes by less than 5%. The pair production in the primary process, which is independent of the detector material has been subtracted, as well as the contamination due to delta rays. The overall systematic error was considered to be 10%. The estimated mean conversion probabilities are 10.9±1.2% and 19.9±2.6% respectively in the barrel and in the forward region.

The detection efficiency for high energy gammas was estimated using an $e^+e^- \rightarrow \gamma\gamma(\gamma)$ simulation [8] and a sample of Bhabha events. The calculated detector efficiency for $e^+e^- \rightarrow \gamma\gamma(\gamma)$ events is 80.6±1.3% and 73.3±2.5% respectively when the two most energetic gammas are in the barrel region or in the forward region. The losses are dominated by the dead regions in θ and ϕ.

The trigger efficiency in the barrel was estimated as the ratio of the number of Bhabha events with track as well as electromagnetic energy trigger to the number of Bhabha events with a track trigger. In the forward region the trigger efficiency was estimated using FEMC subtriggers redundancy. The calculated trigger efficiency is 97.6±0.3% for the barrel region and 99.9±0.1% for the forward region.

Table 1 summarizes the integrated luminosity, the number of observed $\gamma\gamma$ events in the barrel, and the corresponding cross sections as a function of the centre of mass energy. The equivalent centre of mass energy of all the observed data, taking into account the luminosity at each energy point and the $1/s$ dependence of the QED cross section, is also given in table 1.

Table 2 summarizes the number of $\gamma\gamma$ events and the corresponding differential cross section as a function of the polar angle, summed over all centre of mass energies.

Radiative effects are usually deconvoluted from the measured $e^+ e^- \rightarrow \gamma\gamma$ cross section to permit easy comparison with the lowest order QED prediction and with the results of previous experiments. Therefore the measured cross sections presented in tables 1 and 2 are after the subtraction of calculated radiative corrections to order α^3 [8].

4 Test of QED

The total and differential cross sections for $e^+e^- \rightarrow \gamma\gamma$ with radiative effects subtracted are compared with the QED prediction in figs. 3 and 4. There is good agreement for the total cross section($\chi^2/NDF = 3.3/7$) as well as for the differential cross section ($\chi^2/NDF = 7.9/5$).

Possible deviations from QED are usually parametrized by modifying the QED differential cross section by introducing the cutoff parameters Λ_+ and Λ_- [3,9]:

$$\frac{d\sigma}{d\Omega} = \frac{\alpha^2}{s}\,\frac{1+cos^2\theta}{1-cos^2\theta}\left(1 \pm \frac{s^2}{2\Lambda_\pm^4}(1-cos^2\theta)\right)$$

A maximum likelihood fit to the experimental data gave lower limits at 95% confidence level of $\Lambda_+ > 113$ GeV and $\Lambda_- > 95$ GeV. An overall normalization error of 3 % due to the systematic errors in luminosity and efficiency was taken into account.

5 Search for Z^0 Decays into $\pi^0\gamma$ and $\eta\gamma$

A deviation of the measured cross section from the QED prediction at Z^0 energies could be interpreted as a signal for the existence of a Z^0 decay with a similar experimental signature such as Z^0 decays into $\pi^0\gamma$ and $\eta\gamma$. The expected number of events for $e^+e^- \rightarrow \gamma\gamma$ in each angular and centre of mass energy bin would then be the sum of the contributions of QED and of this Z^0 decay, the latter being estimated assuming a $1+cos^2\theta$ dependence. The limits on the branching ratios were obtained with a maximum likelihood fit. The 95% confidence limit (BR_l) was defined so that the area under the likelihood curve between BR=0 and BR_l is 95% of the total area above BR=0. An overall normalization error of 3 % was again taken into account.

The estimated global efficiencies and geometrical acceptance for the decays $Z^0 \rightarrow \pi^0\gamma$ and $Z^0 \rightarrow \eta^0\gamma$ are 39±2%, and 21±2% respectively. Only the neutral decay modes of the η^0 are considered. The 95% confidence level limits obtained are BR $(Z^0 \rightarrow \pi^0\gamma) < 1.5 \times 10^{-4}$ and BR $(Z^0 \rightarrow \eta^0\gamma) < 2.8 \times 10^{-4}$.

6 Search for Compositeness

The exchange of an excited electron in the t channel would modify the differential QED cross section. Ref. [3] gives the following expression as a function of the mass of the excited electron (M_{e^*}) and the coupling constant (λ_γ):

$$\frac{d\sigma}{d\Omega} = \frac{\alpha^2}{s}\,\frac{1+cos^2\theta}{1-cos^2\theta}\left(1 + \frac{s^2\lambda_\gamma^2}{2M_{e^*}^4}(1-cos^2\theta)\,H(cos^2\theta)\right)$$

where $H(cos^2\theta) = a[a+(1-cos^2\theta)/(1+cos^2\theta)]/[(1+a)^2-cos^2\theta]$ and $a = 2M_{e^*}^2/s$.

When $M_{e^*}^2 >> s$, $H(cos^2\theta)$ tends to unity and the above expression tends to the parametrization referred to in section 4 with $M_{e^*}^2/\lambda_\gamma = \Lambda_+^2$. A likelihood fit to the full expression was performed. Fig. 5 combines the resulting 95% confidence level limit contour on the (M_{e^*}, λ_γ) plane with the limit contour obtained from DELPHI's search for the t-channel (γ coupling) production of e^*e pairs [10]. While the latter gives a better limit up to the kinematical limit at the Z^0 energy, the $\gamma\gamma$ channel reaches higher values of M_{e^*}. For $\lambda_\gamma = 1$, $M_{e^*} > 100$ GeV.

In some composite models [4], the branching ratio for $Z^0 \to \gamma\gamma\gamma$ can be as high as $2\text{x}10^{-4} < Q^6 >$, where $< Q^6 >$ is the average of the sixth power of the charge of the Z^0 constituents. In other models [11] a scalar partner of the Z^0, called S, is predicted. This boson would couple weakly to fermions but would have a relatively strong coupling to $Z^0\gamma$ and to $\gamma\gamma$. The Z^0 could then decay into S and a monoenergetic γ and the S could decay into $\gamma\gamma$.

Assuming a phase space Z^0 decay into three gammas, the global efficiency and geometrical acceptance for detecting a $\gamma\gamma\gamma$ event is 25±3%. Two $\gamma\gamma\gamma$ events were found. The same two events were the only ones where the two most energetic gammas had an acoplanarity greater than 2^0. The expected number of events from the QED contribution is 1.4±0.2. The kinematical parameters of these events after imposing energy-momentum conservation are indicated in table 3.

A 95% confidence level limit of BR $(Z^0 \to \gamma\gamma\gamma) < 1.4 \times 10^{-4}$ has been determined from the total number of observed and expected $\gamma\gamma\gamma$ events.

7 Summary

The analysis of $e^+e^- \to \gamma\gamma(\gamma)$ shows good agreement with the QED predictions.

Lower limits on the QED cutoff parameters $\Lambda_+ > 113$ GeV ,and $\Lambda_- > 95$ GeV as well as on M_{e^*} as a function of λ_γ were obtained.

Upper limits, at 95% confidence level, were set on the following processes:

- BR $(Z^0 \to \pi^0\gamma) < 1.5 \times 10^{-4}$
- BR $(Z^0 \to \eta^0\gamma) < 2.8 \times 10^{-4}$
- BR $(Z^0 \to \gamma\gamma\gamma) < 1.4 \times 10^{-4}$

Similar results on these channels have been reported recently [12,13,14].

8 Acknowledgements

We are greatly indebted to our technical staff and collaborators and funding agencies for their support in building the DELPHI detector, and to the members of the CERN-SL Division for the speedy commissioning and superb performance of the LEP collider.

REFERENCES

[1] - L.D.Landau, Dokl. Akad. Nauk. URSS 60 (1948) 207.
- C. N. Yang, Phys. Rev. 77 (1950) 242.

[2] - M. Jacob and T. T. Wu, Phys. Lett. B 232 (1989) 529.
- N.G.Deshpande,P.B.Pal and F.I.Olness, Phys.Lett.B241(1990)119.
- L.Arnellos,W.J.Marciano and Z.Parsa,Nucl.Phys.B196(1982)378.
- E.W.N.Glover and J.J.van der Bij, CERN 89-08 v.2 p.1.

[3] - A.Litke, Harvard Univ., Ph.D. Thesis (1970), unpublished.
- Compositeness at LEP II - D.Treille et al., ECFA 87-108, CERN 87-08, Volume 2, p.414.

[4] - Compositeness Working Group - F. Renard et al., CERN 89-08, Volume 2, p.185.

[5] - DELPHI Collaboration, P.Abreu et al., CERN-PPE/90-167.

[6] - DELPHI Collaboration, Nucl. Inst. Meth. A303 (1991) 233.

[7] - DELPHI Collaboration, P.Abreu et al, Phys.Lett. B 231 (1989) 538 and B 241 (1990) 435.

[8] - F.A. Berends and R.Kleiss, Nucl. Phys. B 186 (1981) 22.

[9] - S.Drell, Ann. Phys. (N.Y.) 4 (1985) 75.
F.E.Low, Phys. Rev. Lett. 14 (1965) 238.

[10] - Search for Excited Leptons in Z^0 Decays
DELPHI Collaboration, P.Abreu et al.,.in preparation

[11]- F.M. Renard, Phys. Lett. B126 (1983) 59.

[12]- ALEPH Collaboration, D.Decamp et al., Phys. Lett. B241 (1990) 635.

[13]- OPAL Collaboration, M.Z.Akrawy et al., Phys. Lett. B257 (1990) 531.

[14]- L3 Collaboration, B.Adeva et al., Phys. Lett. B250 (1990) 199.

Table 1

Energy distribution of $\gamma\gamma$ events

The σ_0 values are the QED lowest order predictions and the σ values are the measured cross sections after radiative effects have been subtracted

$\sqrt{s}(GeV)$	barrel			
	$\mathcal{L}(nb^{-1})$	$N_{\gamma\gamma}$	$\sigma_0(pb)$	$\sigma(pb)$
88.22	326.6	3	19.62	12.6± 7.7
89.22	355.4	3	19.18	11.6± 7.0
90.22	372.5	5	18.76	18.4± 8.8
91.22	2450.8	28	18.35	15.6± 3.5
92.22	393.9	5	17.95	17.4± 8.3
93.22	312.6	6	17.57	26.3±11.6
94.22	456.8	5	17.20	15.0± 7.2
91.25	4668.6	55	18.34	16.1± 2.7

Table 2

Angular distribution of $\gamma\gamma$ events

The $d\sigma_0/d\Omega$ values are the QED lowest order predictions and $d\sigma/d\Omega$ values are the measured differential cross sections after radiative effects have been subtracted

$\cos\theta$	$\mathcal{L}(pb^{-1})$	$N_{\gamma\gamma}$	$d\sigma_0/d\Omega(pb/sr)$	$d\sigma/d\Omega(pb/sr)$
0.00 - 0.20	4.67	12	2.56	3.3± 1.1
0.20 - 0.40	4.67	17	3.01	3.7± 1.0
0.40 - 0.60	4.67	12	4.22	2.7± 0.9
0.60 - 0.74	4.67	14	6.71	4.5± 1.4
0.82 - 0.87	3.66	7	15.32	9.8± 4.3

Table 3

Kinematical parameters of $\gamma\gamma\gamma$ events

Energies are given in GeV and angles in degrees

Event	$\sqrt{s}$	E_1	E_2	E_3	*Acop*	*Acol*
1	94.22	43.9	34.6	15.7	5.6	18.6
2	92.22	39.8	39.0	13.4	23.2	19.6

FIGURE CAPTIONS

Figure 1: Distribution of the difference $(180^0 - \Delta\phi)$ in azimuthal angle between the two most energetic clusters for the $\gamma\gamma$ and for the Bhabha events : a) Forward region $(29^0 < \Theta < 35^0$ b) Barrel region. The relative number of Bhabha and $\gamma\gamma$ events are not normalized.

Figure 2: Acollinearity (a) and acoplanarity (b) distributions for the two most energetic clusters of the 64 $\gamma\gamma(\gamma)$ candidates (histogram) compared with the QED prediction (solid points). The $\gamma\gamma$ events are obtained by imposing an acoplanarity cut at two degrees. Only two events remain above this cut.

Figure 3: Energy dependence of the radiatively corrected cross section for the process $e^+ e^- \rightarrow \gamma\gamma$. The solid line shows the QED prediction.

Figure 4: Angular dependence of the radiatively corrected cross section for the process $e^+ e^- \rightarrow \gamma\gamma$. The solid line shows the QED prediction.

Figure 5: Upper limit on the effective coupling constant λ_γ / M_{e^*} versus M_{e^*}. Below the kinematical limit $M_{e^*} = M_{Z^0}$ a better limit is obtained by the DELPHI search for the t-channel production of e^*e pairs [10]. Above $M_{e^*} = M_{Z^0}$ the limit comes from the present study of $e^+e^- \rightarrow \gamma\gamma$.

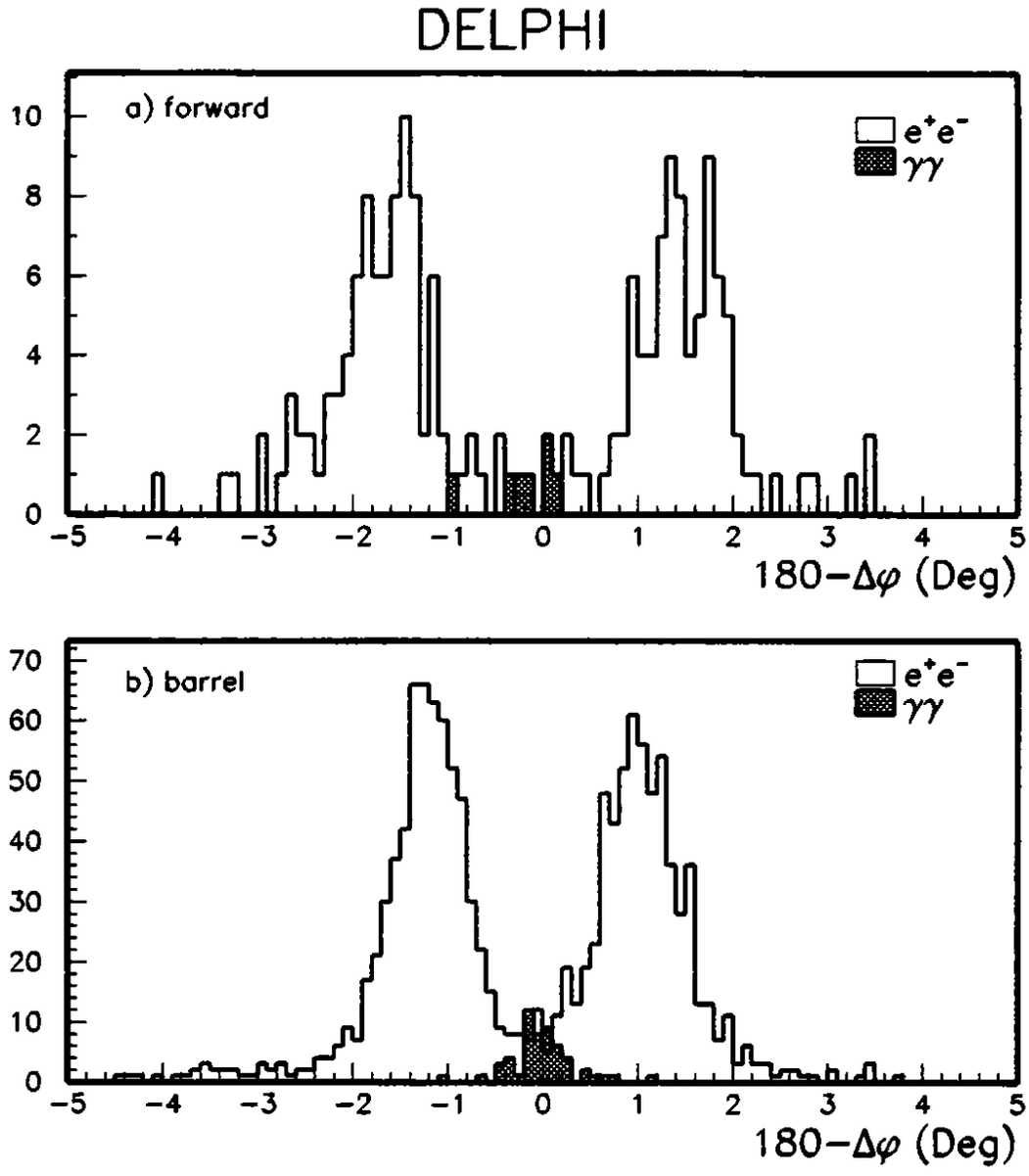
DELPHI
a) forward
e^+e^-
$\gamma\gamma$
10
8
6
4
2
0
−5
−4
−3
−2
−1
0
1
2
3
4
5
180−Δφ (Deg)
b) barrel
e^+e^-
$\gamma\gamma$
70
60
50
40
30
20
10
0
−5
−4
−3
−2
−1
0
1
2
3
4
5
180−Δφ (Deg)

fig. 1

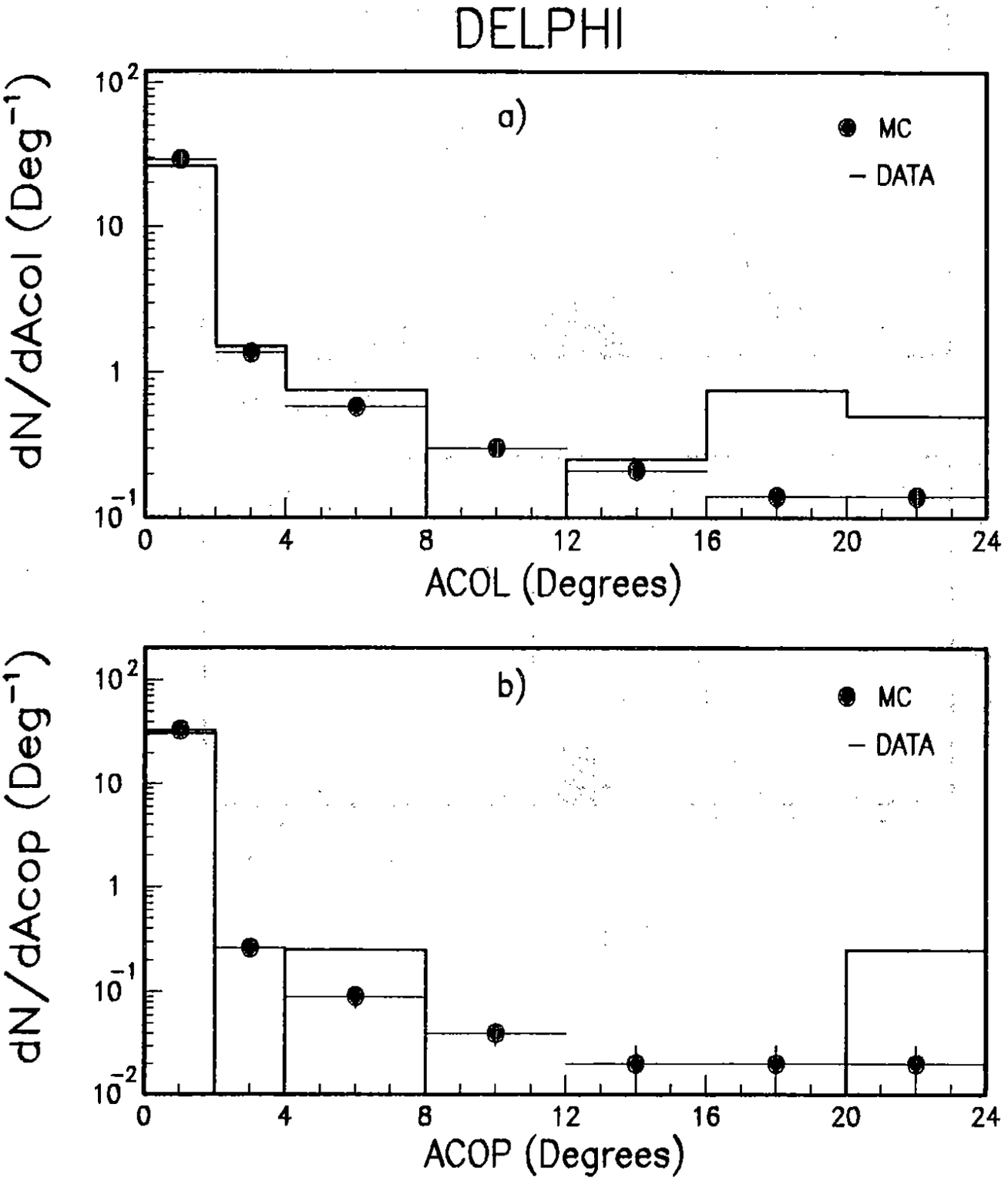
DELPHI
a)
MC
DATA
dN/dAcol (Deg^{-1})
ACOL (Degrees)
b)
MC
DATA
dN/dAcop (Deg^{-1})
ACOP (Degrees)

fig. 2

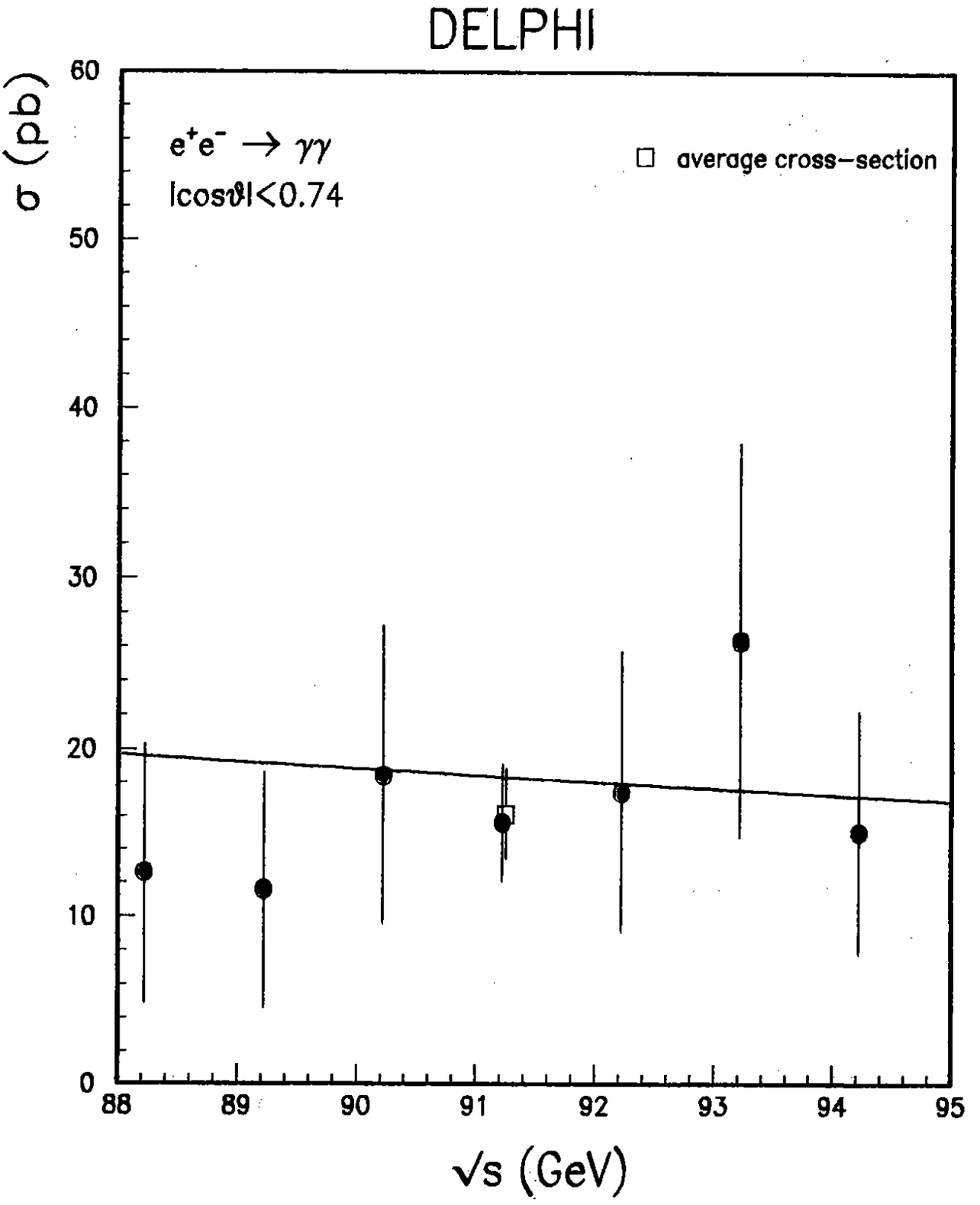
DELPHI
σ (pb)
$e^+e^- \rightarrow \gamma\gamma$
$|\cos\vartheta|<0.74$
average cross-section
60
50
40
30
20
10
0
88
89
90
91
92
93
94
95
√s (GeV)

fig. 3

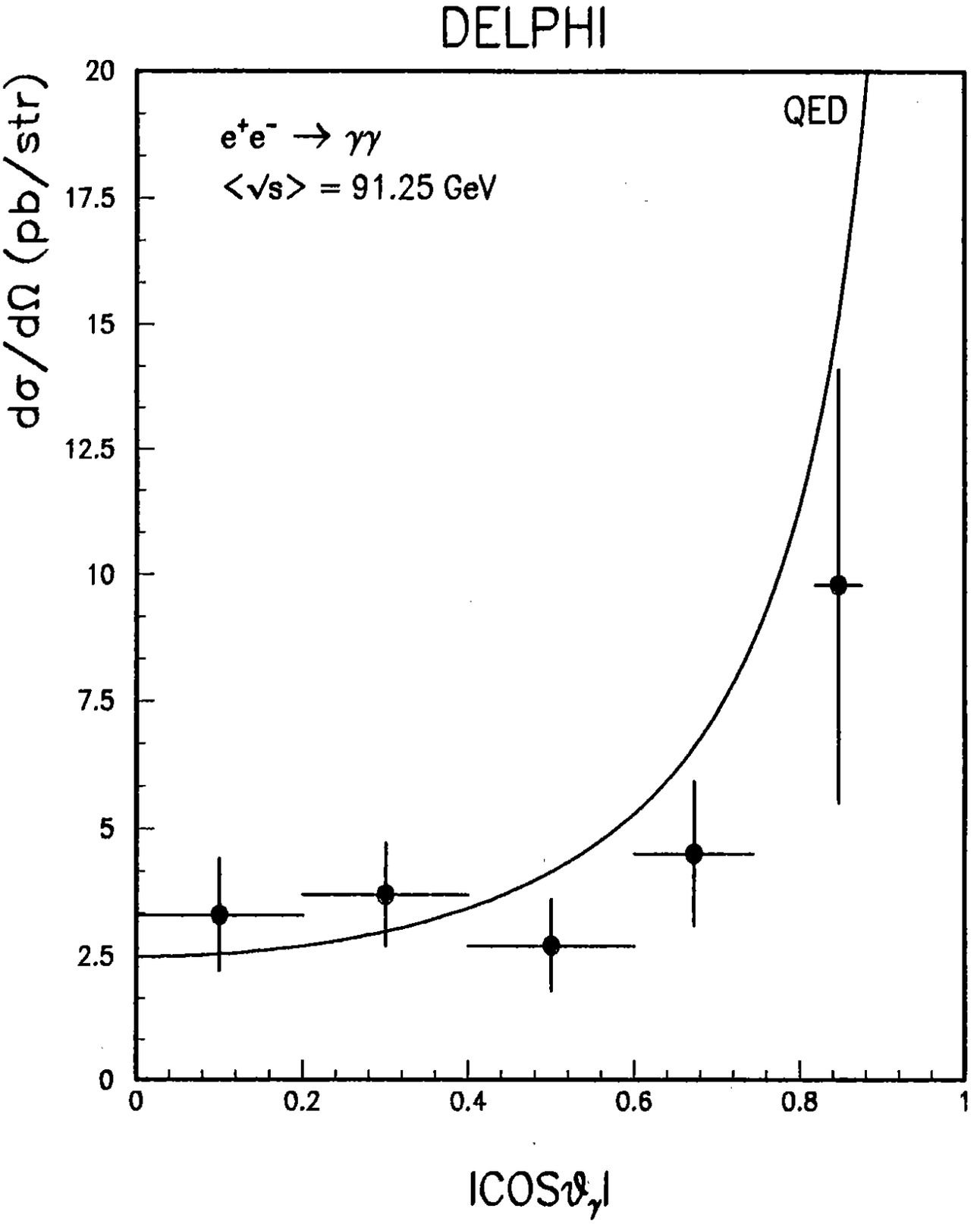
DELPHI
$e^+e^- \rightarrow \gamma\gamma$
<√s> = 91.25 GeV
QED
dσ/dΩ (pb/str)
20
17.5
15
12.5
10
7.5
5
2.5
0
0
0.2
0.4
0.6
0.8
1
|COSϑγ|

fig. 4

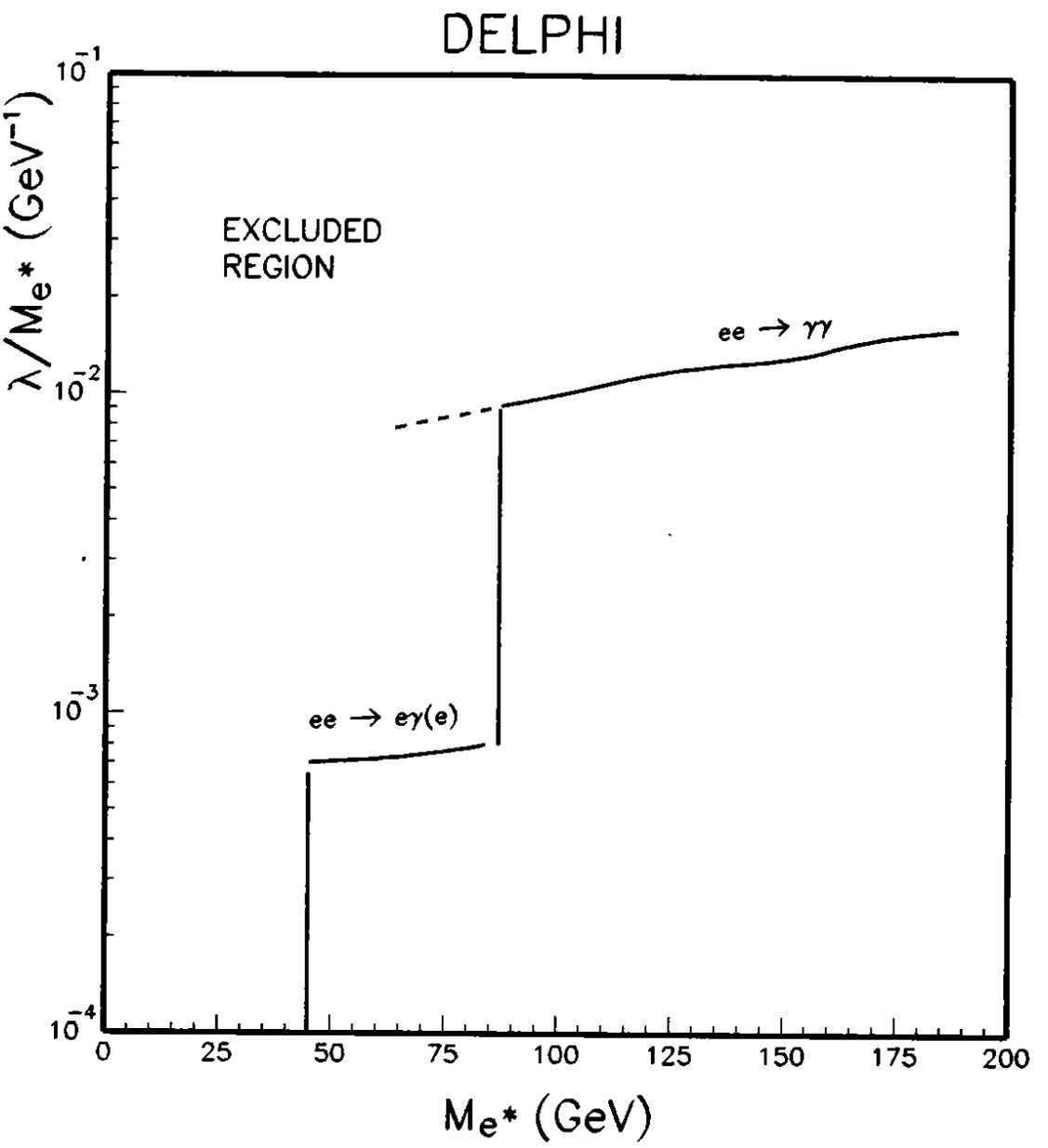

fig. 5

Imprimé au CERN. Prix: 0.55 Fr.